Journal of Innovative Optical Health Sciences
Vol. 8, No. 3 (2015) 1541006 (10 pages)

DOI: 10.1142/S1793545815410060

World Scientific
www.worldscientific.com

Quantification of glucose and glycerol diffusion in myocardium

Daria K. Tuchina*,§, Alexey N. Bashkatov*, Elina A. Genina*
and Valery V. Tuchin*,†,‡
*Research-Educational Institute of Optics and Biophotonics
Saratov State University, Saratov 410012, Russia
†Laboratory of Laser Diagnostics of Technical and Living Systems
Institute of Precise Mechanics and Control RAS
Saratov 410028, Russia
‡Optoelectronics and Measurement Techniques Laboratory
P. O. Box 4500, University of Oulu FIN-90014, Oulu, Finland
§tuchinadk@mail.ru

Received 27 March 2014
Accepted 11 September 2014
Published 15 October 2014

The results on determination of glucose and glycerol diffusion coefficients in myocardium tissue are presented. The method is based on the measurement and analysis of temporal dependence of tissue optical collimated transmittance under action of a hyperosmotic agent. This temporal tissue response is related to the rate of the agent and water diffusion in a tissue. The diffusion coefficients for tissue fluid fluxes at glucose and glycerol application to the myocardium at 20°C have been estimated as $(4.75 \pm 3.40) \times 10^{-7}$ and $(7.71 \pm 4.63) \times 10^{-7}$ cm^2/s, respectively.

Keywords: Diffusion coefficient; optical clearing; dehydration; scattering.

1. Introduction

Recent technological advancements in the photonics industry have led to a resurgence of interest in optical imaging and stimulated a real progress toward the development of noninvasive clinical functional imaging techniques. Application of the optical methods for physiological-condition monitoring and cancer diagnostics, as well as for treatment, is a growing field due to their simplicity, low cost and low risk. In clinical dermatology, oncology, gastroenterology, gynecology, and other medical fields, optical methods are widely used for vessel imaging, detection, localization and treatment of malignant growths using photothermal or photodynamic therapy. Frequently, the optical methods use dyes and drugs for cell sensitizing and enhancement of the local immune status of a tissue,[1,2] therefore the development of noninvasive measurement techniques for monitoring of exogenous and endogenous (metabolic) agents in human tissues

and determination of their diffusivity are very important for diagnosis and therapy of various human diseases.[3,4]

Cardiovascular disease is the cause of numerous deaths with an estimated 17.3 million deaths worldwide each year, accounting for some 30% of all deaths.[5] The number of people who die from cardiovascular diseases, mainly from heart disease and stroke, will increase to reach 23.3 million by 2030.[5,6] Cardiovascular diseases are projected to remain the single leading cause of death.[6] Along with conventional methods, many optical methods are rapidly developing to be used in nearest future for diagnostics and therapeutics in cardiology.[7–10]

However, in spite of numerous benefits in the use of optical methods in medicine there are some serious disadvantages. One of the problems is connected with the transport of the light beam through the turbid tissues to the target region of the search or treatment. Due to low absorption and much higher scattering of visible and NIR radiation at propagation within tissues, there are essential limitations on spatial resolution and light penetration depth for optical diagnostic and therapeutic methods to be successfully applied.[3] Control of the tissue optical properties is a very appropriate way to solve the problem. The temporary selective optical clearing of tissue layers is the key technique for structural and functional imaging, particularly for detection of local morphological or physiological inhomogeneities hidden within a highly scattering medium.[3,4,11–17] The optical clearing of biological tissue is based on partial replacement of tissue interstitial fluid by immersion agent with refractive index higher than the refractive index of interstitial fluid and tissue dehydration. These molecular processes, related to phenomenon of osmoses, lead to the matching of refractive indices of the interstitial fluid and tissue structures (collagen fibers, cell organelles, etc.), lesser tissue layer thickness, and better ordering of these structures which cause reduction of light scattering efficiency and increase of scattering anisotropy. Many publications have been dedicated to the investigation of optical clearing of a broad variety of tissues *in vitro*, *ex vivo*, and *in vivo*. Most of them are overviewed in Refs. 3, 4, 11–17 and recent ones present optical clearing of tissues such as skin,[18–32] sclera,[33–35] and skeletal muscle.[36–41] We have found that only in two papers optical clearing of heart tissues were investigated.[42,43] Authors of Ref. 42 have studied the influence of a highly concentrated glycerol on the optical clearing, mechanical reversibility, and thermal damage susceptibility of myocardium and epicardium, and authors of Ref. 43 used a mineral oil/glycerol mixture for optical clearing of archive-compatible paraffin embedded mouse tissues of many types, including heart tissue, with the aim of multiphoton microscopy.

Many different optical clearing agents (OCAs) including the most common, glycerol, glucose, fructose, mannitol, ethylene glycol, propylene glycol, polyethylene glycol, mineral oil, together with chemical enhancers of OCA permeability, DMSO, propylene glycol, thiazone and some others, are used.[3–43] As it follows from the cited literature, glucose and glycerol are the most widely used solutions for the control of tissue scattering properties. The range of concentrations of the chemicals varies from 20% to 54% glucose water solutions and from 20%-glycerol water solution to 100% glycerol. However, the optimal for optical clearing concentration of glucose is around 40% and glycerol is 50–70%.

In spite of the more or less intensive studies of optical clearing efficiency of skeletal muscle[36–41] and a few studies on cardiovascular muscle tissue,[42,43] diffusion coefficients neither for glucose nor glycerol in the myocardium have not been measured yet. The knowledge of diffusion coefficients for OCA–water fluxes in tissues allows one to understand the optical clearing mechanisms more precisely, to improve the mathematical models describing the interaction of the OCAs with the tissue. From practical point of view, this gives the possibility to predict the rate of optical clearing and time period needed to wash out OCA afterward, as well as to develop effective optical clearing compositions for medical application.

In the study, we present for the first time the experimental data for diffusion coefficients of glucose- and glycerol-water fluxes in porcine myocardium.

2. Materials and Methods

2.1. *Optical clearing agents*

As OCAs, aqueous 40%-glucose solution ("Novosibchempharm", Novosibirsk, Russia) and aqueous 58%-glycerol solution were used in this investigation. The 58%-glycerol solution was prepared by mixing glycerol ("Warehouse of chemical reagents

No. 1," Staraya Kupavna, Russia) and distilled water. The refractive indices of glucose and glycerol solutions were measured by Abbe refractometer at 589 nm as $n_{gluc} = 1.391$ and $n_{glyc} = 1.414$, respectively.

2.2. *Tissue samples*

A total of 20 myocardium samples obtained from fresh porcine heart were used in these experiments. Each group of 10 samples was examined during the administration of the aqueous 40%-glucose and 58%-glycerol solutions. Thin samples with about $15 \times 20\,mm^2$ area were cut by ceramic knife and their thickness were measured before and after experiments with a micrometer (precision of $\pm 50\,\mu m$) in five points and averaged. The weight of the samples was measured before and after experiments using electronic balance (SCIENTECH, SA210, USA) with precision of 1 mg.

Myocardium is a special form of striated muscle tissue of the heart. The cell membrane of muscle fibers is sarcolemma, it is filled by intracellular fluid called sarcoplasm that contains myoglobin, which binds the molecules of oxygen diffused from interstitial fluid into muscle fibers. Myoglobin is the main absorber in the muscles. The maximum wavelengths of myoglobin absorption in horses and whales are 435, 560, 434 and 556 nm, respectively. The cardiac muscle sarcoplasm is comprised of myofibrils as a skeletal muscle. Myofibrils are 0.5–2 μm in diameter, the comparable sizes to the visible and near infrared wavelengths indicate Mie scattering to be dominant. Myofibrils mainly consist of protein filaments such as actin and myosin. Sarcoplasm also contains large amounts of glycosomes (granules of stored glycogen). The complex fiber structure causes a strong light scattering of the myocardium.[44–49]

Refractive index values measured for human and bovine myocardium tissue,[3,50] porcine[51–55] and human skeletal muscle tissue[56] are summarized in Table 1. Since the values are very close to each other and weakly dependent on the wavelength in the range under study (600–900 nm), in this paper we assume the average value of refractive index of myocardium tissue as 1.376 ± 0.007. Refractive index of sarcoplasm was estimated as 1.350 and effective refractive index of proteins in muscle tissue — as 1.530.[57] Volume fraction of sarcoplasm was taken as 0.875.[57]

Table 1. Refractive indices of muscle tissue.

Tissue	Refractive index	Wavelength (nm)	Reference
Human myocardium	1.38	456–1064	3, 50
Bovine myocardium	1.38	589	3, 50
Porcine skeletal muscle	1.38 ± 0.007	632.8	51
	1.371	632.8	52
	1.364 ± 0.001	632.8	53
	1.367 ± 0.002	632.8	54
	1.380 ± 0.002	632.8	55
Human skeletal muscle	1.382 ± 0.007	1300	56
Averaged	1.376 ± 0.007		

Note: ± - standard deviation.

2.3. *Experimental setup*

The measurements of collimated transmittance spectra of tissue samples were performed using commercially available spectrometer USB4000-Vis-NIR (Ocean Optics, USA) in the spectral range from 400 to 1000 nm. For the measurements, the 5 mL glass cuvette with tissue sample, fixed on the special plastic plate and immersed in the OCA, was placed between two optical fibers (QP400-1-Vis-NIR, Ocean Optics, USA; 400 μm core diameter) with collimators 74-ACR (Ocean Optics, USA). The halogen lamp HL-2000 (Ocean Optics, USA) was used as a light source. The spectra were recorded every 2–5 min during 90 min for glucose solution and during 40–60 min for solution of glycerol. The measurements were performed at room temperature about 20°C.

2.4. *Estimation of glucose and glycerol diffusion coefficients*

The method of estimation of immersion liquid diffusion coefficient used in this study is based on the measurement of time dependence of tissue optical collimated transmittance, which is related to rate of the chemicals diffusion within a tissue sample.[58]

The problem is solved in the framework of the free diffusion model. Geometrically, the tissue sample can be presented as an infinite plane-parallel slab with finite thickness. Since the cross section of the experimental samples was about 15×20 mm, which is >10-fold bigger than the thickness of the samples, the one-dimensional diffusion problem has

been solved. The one-dimensional diffusion equation has the form[58]:

$$\frac{\partial C(x,t)}{\partial t} = D\frac{\partial^2 C(x,t)}{\partial x^2}, \tag{1}$$

where $C(x,t)$ is the OCA concentration in myocardium tissue sample, g/mL; D is the diffusion coefficient, cm^2/s; t is time of diffusion, s; x is the spatial coordinate, cm.

We suppose that penetration of the immersion liquids into a tissue sample does not change the immersion liquid concentration in the cuvette. This requirement has been met in the experiments since the immersion liquid volume in the cuvette was about 3000 mm^3 and the volume of the myocardium samples was less than 250 mm^3. The corresponding boundary conditions are:

$$C(0,t) = C(l,t) = C_0 = \text{const}, \tag{2}$$

where C_0 is the concentration of the OCA in the cuvette, g/mL; l is the thickness of the sample, cm.

The initial conditions correspond to the absence of the OCA inside the myocardium tissue before its incubation in the immersion liquid:

$$C(x,0) = 0. \tag{3}$$

The volume-average concentration of immersion liquid in the myocardium sample is the solution of Eq. (1) with the boundary Eq. (2) and initial Eq. (3) conditions[58]:

$$C(t) = C_0\left(1 - \frac{8}{\pi^2}\sum_{i=0}^{\infty}\frac{1}{(2i+1)^2}\exp(-(2i+1)^2 t\pi^2 D/l^2)\right). \tag{4}$$

In a first-order approximation, the Eq. (4) is reduced to:

$$C(t) \approx C_0(1 - \exp(-t\pi^2 D/l^2)) = C_0(1 - \exp(-t/\tau)), \tag{5}$$

where $\tau = l^2/(\pi^2 D)$ is the characteristic diffusion time. This approximation gives results close to the exact solution Eq. (4) in the limits of experimental errors, but reduces significantly to a calculation time, especially for the inverse problem solving.

The temporal dependence of the refractive index of the tissue interstitial fluid (n_I) can be found using the law of Gladstone and Dale,[59] which states that for a multi-component system the resulting value of the refractive index represents an average of the refractive indices of the components related to their volume fractions:

$$n_I(t) = (1 - C(t))n_{\text{base}} + C(t)n_{\text{oca}}, \tag{6}$$

where n_{base} is a refractive index of the interstitial fluid at $t = 0$; n_{oca} is a refractive index of the OCA.

The tissue sample model is presented as a slab with a thickness l, which consists of scattering cylinders (myofibrils). The scattering coefficient of the myocardium sample is estimated as[3]:

$$\mu_s = N\frac{\pi^2 a x^3}{8}(m^2-1)^2\left(1 + \frac{2}{(m^2+1)^2}\right), \tag{7}$$

where $N = \varphi/(\pi a^2)$ is the number of the scattering particles (myofibrils) per unit area; φ is the volume fraction of the tissue scatterers; a is the radius of scattering particles; $m = n_s/n_I$ is the ratio of the refractive indices of the particle (n_s) and surrounding medium (n_I), and $x = 2\pi a n_I/\lambda$ is the size parameter, where λ is a wavelength, nm.

The time-dependent collimated transmittance of the sample is defined as:

$$T_c(t) = (1 - r_s)^2\exp(-(\mu_a + \mu_s(t))l), \tag{8}$$

where r_s is the specular reflection coefficient, μ_a and μ_s are the absorption and scattering coefficients, respectively.

This set of equations represents the direct problem, i.e., describes the temporal evaluation of the collimated transmittance of a tissue sample dependent on glucose or glycerol concentration in interstitial fluid. On the basis of measurement of the temporal evolution of the collimated transmittance, the reconstruction of the diffusion coefficient of an OCA in myocardium has been carried out. The inverse problem solution has been obtained by minimization of the target function:

$$f(D) = \sum_{i=1}^{N_t}(T_c(D,t_i) - T_c^*(t_i))^2, \tag{9}$$

where $T_c(D,t)$ and $T_c^*(t)$ are the calculated and experimental values of the time-dependent collimated transmittance, respectively, and N_t is the sampling number. To minimize the target function, the Levenberg–Marquardt nonlinear least-squares-fitting algorithm is described in detail by Press *et al.*[60] has been used. Iteration procedure repeats until experimental and calculated data are

matched. As a termination condition of the iteration process, we have used the following expression:

$$\frac{1}{N_t}\sum_{i=1}^{N_t}\frac{|T_c(D,t_i)-T_c^*(t_i)|}{T_c^*(t_i)}\leq 0.01.$$

3. Results and Discussion

Collimated transmittance spectra of myocardium tissue samples were measured concurrently with administration of glucose or glycerol solutions. The collimated transmittance spectra of myocardium sample during interaction with 40%-glucose solution are shown in Fig. 1. It is seen that the tissue sample is poorly transparent at first few minutes of sample immersion in glucose solution. Next 30 min the transmittance has increased significantly. Myocardium sample becomes more transparent because of glucose molecules permeation into tissue and water molecules diffusion from the tissue, that results in refractive index matching of tissue components and tissue thickness decrease.

The spectra were used to obtain time-dependence of collimated transmittance of myocardium tissue during immersion in 40%-glucose solution. The experimental and calculated temporal dependences of collimated transmittance of the myocardium sample are presented in Fig. 2. Figure 2 shows at the beginning (0–4 min) slow and then faster (4–40 min) increase of collimated transmittance. After 40 min, optical clearing efficiency is saturated.

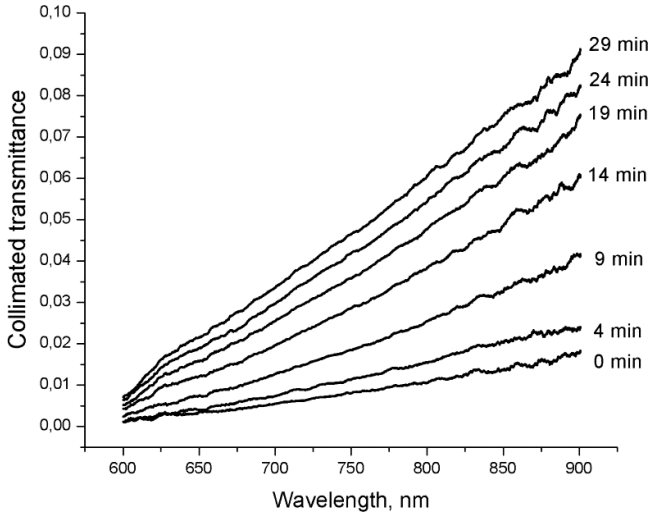

Fig. 1. The typical spectra of collimated transmittance of the myocardium sample measured at different time intervals concurrently with administration of 40%-glucose solution.

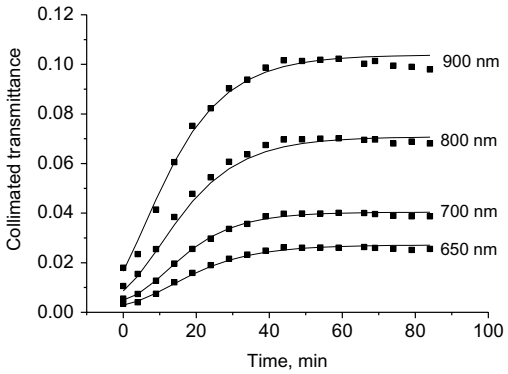

Fig. 2. The experimental (dots) and calculated (lines) time dependences of collimated transmittance of the myocardium sample placed in the 40%-glucose solution.

The average value of sample thickness before immersion in glucose solution was 0.66 ± 0.13 mm, and after immersion was 0.58 ± 0.19 mm. However, the difference in the sample thickness ($\sim 80\,\mu$m) is comparable with the precision of our thickness measurements ($\pm 50\,\mu$m) and therefore for the calculation of the diffusion coefficients, the tissue thickness decrease has not been taken into account. The weight of the samples was also measured before and after immersion in the glucose solution. On average, the weight of the samples was reduced by 7.8%.

Quantification of glucose diffusion rate for the 10 tissue samples was performed by calculating the temporal dependences for collimated transmittance by using the algorithm described above in the Sec. 2.4. The obtained average value of glucose diffusion coefficient for myocardium tissue is $(4.75 \pm 3.40) \times 10^{-7}$ cm^2/s.

The temporal dependences for collimated transmittance of the myocardium sample at its immersion in 58%-glycerol solution obtained from measured and calculated spectra of the sample using described algorithm are shown in Fig. 3. The rather fast increase of the collimated transmittance is observed during the first 10 min of glycerol solution action. From 10 to 15 min, slow increase of collimated transmittance takes place, and after 15 min optical clearing efficiency is saturated. As a result, the myocardium sample became more optically transparent.

The average value of myocardium sample thickness before immersion in glycerol solution was 0.53 $\pm$ 0.06 mm and after 40–60 min — 0.47 ± 0.03 mm; that suggests tissue dehydration in response to the

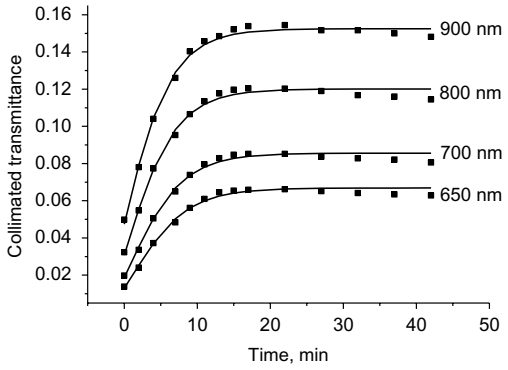

Fig. 3. The experimental (dots) and calculated (lines) time dependences of collimated transmittance of the myocardium sample placed in the 58%-glycerol solution.

action of glycerol solution. However, thickness change of $\sim 60\,\mu$m is comparable with precision of our thickness measurements and therefore for the calculation of the diffusion coefficients, the decrease of the tissue thickness has not been taken into account. On average, at glycerol application the weight of the samples was reduced by 14%.

Estimated values for diffusion and permeation coefficients of glycerol in myocardium tissue are presented in Table 2.

Behavior of the temporal dependence of collimated transmittance of myocardium samples under action of the 40%-glucose and 58%-glycerol solutions is similar, i.e., the tissue transmittance is increasing gradually and then saturated. However, increase of collimated transmittance of myocardium tissue is faster for glycerol administration, it takes about 15 min to reach saturation of optical clearing, whereas in the case of application of 40%-glucose solution the optical clearing saturation is observed after 40–50 min only. Thus, we can see that glycerol molecules penetrate into myocardium faster than glucose. The differences can be connected with differences in viscosity of the solutions and interaction ability of diffusing molecules with tissue components. As it has been presented in Ref. 62, viscosity of 40%-aqueous glucose solution is 63.0 ± 1.1 centipoises, whereas viscosity of 60%-aqueous glycerol solution is of 11 centipoises only.[63] Since diffusion coefficient is directly proportional to viscosity of a penetrating agent, the glycerol solution should have a bigger penetration rate in comparison with the glucose solution.

As it can be seen in Figs. 2 and 3, action of the glucose solution increases myocardium transmittance to 6–7 times, whereas action of the glycerol solution increases the tissue transmittance to 3–4 times only. However, taking into account mean thickness of the samples, we obtain approximately similar decreasing of the tissue scattering coefficient ($\frac{\mu_s(t=0)}{\mu_s(\text{final})} = 1.64 \pm 0.09$ at application of the glucose solution and $\frac{\mu_s(t=0)}{\mu_s(\text{final})} = 1.56 \pm 0.01$ at application of glycerol solution) in the wavelength range. This is an expected result, since refractive indices of these used OCAs are close enough to each other.

The distinction in weight loss of the samples ($\Delta W = 7.8\%$ at application of the glucose solution and 14% at application of the glycerol solution) is connected with the difference in osmotic properties of the glucose and glycerol solutions. Since osmolarity of the glycerol solution is $\sim$ 3-fold larger than osmolarity of the glucose solution, the glycerol solution provided more intensive dehydration effect in comparison with the glucose solution.

Measurements of glucose and glycerol penetration rate into biological tissues (skin dermis, esophagus, breast tissue, etc.) have been performed earlier with the following results: 40%-glucose permeation coefficient for skin is $(1.78 \pm 0.04) \times 10^{-6}$ cm/s,[26] for breast tissue it is $(5.76 \pm 0.89) \times 10^{-6}$ cm/s,[64] and for esophagus is $(1.74 \pm 0.04) \times 10^{-5}$ cm/s.[65] The glucose diffusion coefficient in skeletal muscle and mammalian dermis was estimated as 8.3×10^{-7} cm^2/s[40] and 2.6×10^{-7} cm^2/s,[66] respectively. In this study, we found that glucose diffusion coefficient in myocardium is $(4.75 \pm 3.40) \times 10^{-7}$ cm^2/s (see Table 2) which is twice less than in skeletal muscle, 8.3×10^{-7} cm^2/s.[40]

Table 2. The diffusion and permeation coefficients of glucose and glycerol in myocardium.

Solution	Thickness (mm)	Diffusion coefficient (cm^2/s)	Permeation coefficient (cm/s)[a]
40%-glucose solution	0.66 ± 0.13	$(4.75 \pm 3.40) \times 10^{-7}$	$(8.78 \pm 7.22) \times 10^{-6}$
58%-glycerol solution	0.52 ± 0.06	$(7.71 \pm 4.63) \times 10^{-7}$	$(1.59 \pm 0.99) \times 10^{-5}$

Note: $\pm$ - standard deviation.
[a]The permeation coefficients have been calculated using the relation $P = D/l$.[61]

This difference could be associated with more dense structure of myocardium.

The 60%-glycerol solution permeation coefficient was presented for breast tissues as $(0.89 \pm 0.02) \times 10^{-5}$ cm/s.[67] For human skin, permeation coefficient of 40%-glycerol solution has been estimated as $(1.67 \pm 0.04) \times 10^{-6}$ cm/s.[26]

The difference between the diffusion (permeation) coefficients obtained in this study and the ones presented by the other authors is explained mostly by the differences of structural properties of the investigated tissues. For example, skin and esophagus are more dense tissues than breast, and so, have smaller permeation and diffusion coefficients for both glucose and glycerol. The measured permeation coefficients of myocardium for glucose ($(8.78 \pm 7.22) \times 10^{-6}$ cm/s) and glycerol ($(1.59 \pm 0.99) \times 10^{-5}$ cm/s) solutions are close to measured ones for breast tissue that can be explained by some similarity of their structure, associated with fibrous nature. Some difference can be also due to distinctions in experimental and calculation methods used for estimation of the diffusion and permeation coefficients.

4. Conclusion

It can be concluded that such hyperosmotic immersion liquids such as aqueous glucose and glycerol solutions can be used for effective control of optical properties of myocardium tissue. Due to the interaction of glucose and glycerol molecules with myocardium, a considerable increase of collimated transmittance (6–7 times for glucose and 3–4 times for glycerol) caused by reduction of tissue scattering coefficient are observed.

The optical clearing effect can be used to improve various optical imaging technologies, including linear and multi-photon microscopy, optical coherence tomography, and microscopy, due to increase of probing depth and enhancement of spatial resolution of the techniques.[68]

The collimated transmittance increase happened faster for glycerol administration (~ 15 min) than for 40%-glucose solution (40–50 min). Such a difference indicates that involvement of the water flux, that is faster than diffusion rate of glycerol and glucose molecules, could be different for application of these two OCAs. For 40%-glucose solution, we are expecting much less involvement of the water flux, because there is a balance between free water content in tissues (around 60%) and in applied solution.[41]

The average values of glucose and glycerol diffusion coefficients in myocardium tissue were estimated as $(4.75 \pm 3.40) \times 10^{-7}$ and $(7.71 \pm 4.63) \times 10^{-7}$ cm^2/s, respectively. The obtained results can be used for optimization of tissue optical clearing technique and improvement of biophysical and mathematical models describing interactions between tissues components and chemicals.

Important to note that glycerol/water mixtures have cryoprotective properties for various types of cells, tissues, and organs due to their ability to inhibit ice crystallization that is linked to the concentration of glycerol and the hydrogen bonding patterns formed by these solutions.[69] Therefore, studies of interaction of glycerol–water solution with myocardium done in this paper could also be valuable for the field of cryobiology.

Acknowledgments

The work was carried out under the partial support from grants: 13-02-91176 of Russian Foundation for Basic Research, grant No. 14.Z50.31.0004 by Government of the Russian Federation, Russian Presidential grant NSh-703.2014.2.

References

1. X. Li, M. F. Naylor, H. Le, R. E. Nordquist, T. K. Teague, C. A. Howard, C. Murray, W. R. Chen, "Clinical effects of *in situ* photoimmunotherapy on late-stage melanoma patients: A preliminary study," *Cancer Biol. Ther.* **10**(11), 1081–1087 (2010).
2. X. Li, G. L. Ferrel, M. C. Guerra, T. Hode, J. A. Lunn, O. Adalsteinsson, R. E. Nordquist, H. Liu, W. R. Chen, "Preliminary safety and efficacy results of laser immunotherapy for the treatment of metastatic breast cancer patients," *Photochem. Photobiol. Sci.* **10**(5), 817–821 (2011).
3. V. V. Tuchin, *Tissue Optics: Light Scattering Methods and Instruments for Medical Diagnosis*, Vol. PM166, SPIE Press, Bellingham, WA (2007).
4. V. V. Tuchin, *Optical Clearing of Tissues and Blood*, Vol. PM154, SPIE Press, Bellingham, WA (2005).
5. World Health Organisation, "Global status report on noncommunicable diseases 2010," World Health Organization, Geneva (2011).
6. C. D. Mathers, D. Loncar, "Projections of global mortality and burden of disease from 2002 to 2030," *PLoS Med.* **3**(11), e442 (2006).

7. S. Alali, M. Ahmad, A. Kim, N. Vurgun, M. F. G. Wood, I. A. Vitkin, "Quantitative correlation between light depolarization and transport albedo of various porcine tissues," *J. Biomed. Opt.* **17**(4), 045004 (2012).
8. T. Lindbergh, E. Haggblad, H. Ahn, E. G. Salerud, M. Larsson, T. Stromberg, "Improved model for myocardial diffuse reflectance spectra by including mitochondrial cytochrome aa3, methemoglobin, and inhomogenously distributed RBC," *J. Biophotonics* **4**(4), 268–276 (2011).
9. J. W. Pickering, S. Bosman, P. Posthumus, P. Blokland, J. F. Beek, M. J. C. van Gemert, "Changes in the optical properties (at 632.8 nm) of slowly heated myocardium," *Appl. Opt.* **32**(4), 367–371 (1993).
10. P. Whittaker, M. J. Patterson, "Ventricular remodeling after acute myocardial infarction: Effect of low-intensity laser irradiation," *Lasers Surg. Med.* **27**, 29–38 (2000).
11. V. V. Tuchin, "Optical clearing of tissues and blood using the immersion method," *J. Phys. D: Appl. Phys.* **38**, 2497–2518 (2005).
12. E. A. Genina, A. N. Bashkatov, V. V. Tuchin, "Glucose-induced optical clearing effects in tissues and blood," *Handbook of Optical Sensing of Glucose in Biological Fluids and Tissues*, Chapter 21, V. V. Tuchin (Ed.), pp. 657–692, Taylor & Francis Group LLC, CRC Press (2009).
13. E. A. Genina, A. N. Bashkatov, V. V. Tuchin, "Tissue optical immersion clearing," *Expert Rev. Med. Devices* **7**(6), 825–842 (2010).
14. V. V. Tuchin, M. Leahy, D. Zhu, "Special issue: Optical clearing for biomedical imaging," *J. Innov. Opt. Health Sci.* **3**(3), v–vi (2010).
15. E. A. Genina, A. N. Bashkatov, K. V. Larin, V. V. Tuchin, "Light-tissue interaction at optical clearing," *Laser Imaging and Manipulation in Cell Biology*, Chapter 7, F. S. Pavone (Ed.), pp. 115–164, Wiley-VCH Verlag GmbH & Co. KGaA, Weinheim (2010).
16. K. V. Larin, M. G. Ghosn, A. N. Bashkatov, E. A. Genina, N. A. Trunina, V. V. Tuchin, "Optical clearing for OCT image enhancement and in-depth monitoring of molecular diffusion," *IEEE J. Sel. Top. Quantum Electron.* **18**(3), 1244–1259 (2012).
17. D. Zhu, K. V. Larin, Q. Luo, V. V. Tuchin, "Recent progress in tissue optical clearing," *Laser Photon. Rev.* **7**(5), 732–757 (2013).
18. E. A. Genina, A. N. Bashkatov, A. A. Korobko, E. A. Zubkova, V. V. Tuchin, I. Yaroslavsky, G. B. Altshuler, "Optical clearing of human skin: Comparative study of permeability and dehydration of intact and photothermally perforated skin," *J. Biomed. Opt.* **13**(2), 021102 (2008).
19. A. K. Bui, R. A. McClure, J. Chang, C. Stoianovici, J. Hirshburg, A. T. Yeh, B. Choi, "Revisiting optical clearing with dimethyl sulfoxide (DMSO)," *Lasers Surg. Med.* **41**, 142–148 (2009).
20. Z. Zhi, Z. Han, Q. Luo, D. Zhu, "Improve optical clearing of skin *in vitro* with propylene glycol as a penetration enhancer," *J. Innov. Opt. Health Sci.* **2**(3), 269–278 (2009).
21. C. Liu, Z. Zhi, V. V. Tuchin, Q. Luo, D. Zhu, "Enhancement of skin optical clearing efficacy using photo-irradiation," *Lasers Surg. Med.* **42**, 132–140 (2010).
22. J. Yoon, D. Park, T. Son, J. Seo, J. S. Nelson, B. Jung, "A physical method to enhance transdermal delivery of a tissue optical clearing agent: Combination of microneedling and sonophoresis," *Lasers Surg. Med.* **42**, 412–417 (2010).
23. H. Zhong, Z. Guo, H. Wei, C. Zeng, H. Xiong, Y. He, S. Liu, "*In vitro* study of ultrasound and different-concentration glycerol-induced changes in human skin optical attenuation assessed with optical coherence tomography," *J. Biomed. Opt.* **15**(3), 036012 (2010).
24. X. Wen, Z. Mao, Z. Han, V. V. Tuchin, D. Zhu, "*In vivo* skin optical clearing by glycerol solutions: Mechanism," *J. Biophotonics* **3**(1–2), 44–52 (2010).
25. J. Wang, Y. Liang, S. Zhang, Y. Zhou, H. Ni, Y. Li, "Evaluation of optical clearing with the combined liquid paraffin and glycerol mixture," *Biomed. Opt. Express* **2**(8), 2329–2338 (2011).
26. X. Guo, Z. Guo, H. Wei, H. Yang, Y. He, S. Xie, G. Wu, X. Deng, Q. Zhao, L. Li, "*In vivo* comparison of the optical clearing efficacy of optical clearing agents in human skin by quantifying permeability using optical coherence tomography," *Photochem. Photobiol.* **87**, 734–740 (2011).
27. T. Yu, X. Wen, V. V. Tuchin, Q. Luo, D. Zhu, "Quantitative analysis of dehydration in porcine skin for assessing mechanism of optical clearing," *J. Biomed. Opt.* **16**(9), 095002 (2011).
28. X. Wen, S. L. Jacques, V. V. Tuchin, D. Zhu, "Enhanced optical clearing of skin *in vivo* and optical coherence tomography in-depth imaging," *J. Biomed. Opt.* **17**(6), 066022 (2012).
29. R. He, H. Wei, H. Gu, Z. Zhu, Y. Zhang, X. Guo, T. Cai, "Effects of optical clearing agents on non-invasive blood glucose monitoring with optical coherence tomography: A pilot study," *J. Biomed. Opt.* **17**(10), 101513 (2012).
30. H. Shan, Y. Liang, J. Wang, Y. Li, "Study on application of optical clearing technique in skin diseases," *J. Biomed. Opt.* **17**(11), 115003 (2012).
31. D. Huang, W. Zhang, H. Zhong, H. Xiong, X. Guo, Z. Guo, "Optical clearing of porcine skin tissue

in vitro studied by Raman microspectroscopy," *J. Biomed. Opt.* **17**(1), 015004 (2012).
32. E. A. Genina, A. N. Bashkatov, E. A. Kolesnikova, M. V. Basco, G. S. Terentyuk, V. V. Tuchin, "Optical coherence tomography monitoring of enhanced skin optical clearing in rats *in vivo*," *J. Biomed. Opt.* **19**(2), 021109 (2014).
33. M. G. Ghosn, E. F. Carbajal, N. A. Befrui, V. V. Tuchin, K. V. Larin, "Differential permeability rate and percent clearing of glucose in different regions in rabbit sclera," *J. Biomed. Opt.* **13**(2), 021110 (2008).
34. A. A. Alekhin, A. A. Ionin, S. E. Kozhushko, I. M. Kourylyova, S. I. Kudryashov, K. K. Kuz'min, V. G. Likhvansteva, M. V. Samoylov, L. V. Seleznev, D. V. Sinitsyn, S. D. Zakharov, "*In vitro* femtosecond laser subsurface micro-disruption inside human cornea and pre-cleared sclera," *Laser Phys. Lett.* **7** (6), 463–466 (2010).
35. R. T. Zaman, N. Rajaram, B. S. Nichols, H. G. Rylander III, T. Wang, J. W. Tunnell, A. J. Welch, "Changes in morphology and optical properties of sclera and choroidal layers due to hyperosmotic agent," *J. Biomed. Opt.* **16**(7), 077008 (2011).
36. R. LaComb, O. Nadiarnykh, S. Carey, P. J. Campagnola, "Quantitative second harmonic generation imaging and modeling of the optical clearing mechanism in striated muscle and tendon," *J. Biomed. Opt.* **13**(2), 021109 (2008).
37. O. Nadiarnykh, P. J. Campagnola, "Retention of polarization signatures in SHG microscopy of scattering tissues through optical clearing," *Opt. Express* **17**(7), 5794–5806 (2009).
38. R. Liao, N. Zeng, D. Li, T. Yun, Y. He, H. Ma, "A study on penetration depth of polarization imaging," *J. Innov. Opt. Health Sci.* **3**(3), 177–181 (2010).
39. L. Oliveira, A. Lage, M. P. Clemente, V. Tuchin "Rat muscle opacity decrease due to the osmosis of a simple mixture," *J. Biomed. Opt.* **15**(5), 055004 (2010).
40. L. Oliveira, M. I. Carvalho, E. Nogueira, V. V. Tuchin, "Optical measurement of rat muscle samples under treatment with ethylene glycol and glucose, *J. Innov. Opt. Health Sci.* **6**(2), 1350012 (2013).
41. L. M. Oliveira, M. I. Carvalho, E. Nogueira, V. V. Tuchin, "The characteristic time of glucose diffusion measured for muscle tissue at optical clearing," *Laser Phys.* **23**(7), 075606 (2013).
42. P. B. Wells, A. T. Yeh, J. D. Humphrey, "Influence of glycerol on the mechanical reversibility and thermal damage susceptibility of collagenous tissues," *IEEE Trans. Biomed. Eng.* **53**(4), 747–753 (2006).
43. J. W. Wilson, S. Degan, W. S. Warren, M. C. Fischer, "Optical clearing of archive-compatible paraffin embedded tissue for multiphoton microscopy," *Biomed. Opt. Express* **3**(11), 2752–2760 (2012).
44. M. Frotscher, W. Kahle, *Color Atlas and Textbook of Human Anatomy*, 6th Edition, Georg Thieme Verlag, Stuttgart, New York (2010).
45. V. Sankaran, D. J. Maitland, J. T. Walsh (Jr.), "Polarized light propagation in turbid media," *Proc. SPIE* **3598**, 158–165 (1999).
46. J. A. G. Rhodin, *Histology. A Text and Atlas*, Oxford University Press, New York (1974).
47. S. Bosman, "Heat-induced structural alterations in myocardium in relation to changing optical properties," *Appl. Opt.* **32**(4), 461–463 (1993).
48. R. G. Kessel, *Basic Medical Histology: The Biology of Cells, Tissues, and Organs*, Oxford University Press, New York (1998).
49. A. Douplik, G. Saiko, I. Schelkanova, V. V. Tuchin, "The response of tissue to laser light," *Lasers for Medical Application*, Chapter 2, H. Jelinkova (Ed.), Woodhead Publishing (2012).
50. H.-J. Schwarzmaier, A. N. Yaroslavsky, A. Terenji, S. Willmann, I. V. Yaroslavsky, T. Kahn, "Changes in the optical properties of laser coagulated and thermally coagulated bovine myocardium," *Proc. SPIE* **3254**, 361–365 (1998).
51. H. Li, S. Xie, "Measurement method of the refractive index of biotissue by total internal reflection," *Appl. Opt.* **35**(10), 1793–1795 (1996).
52. J.-C. Lai, Y.-Y. Zhang, Z.-H. Li, H.-J. Jiang, A.-Z. He, "Complex refractive index measurement of biological tissues by attenuated total reflection ellipsometry," *Appl. Opt.* **49**(16), 3235–3238 (2010).
53. H. Li, S. Xie, L. Lin, "Refractive index of biotissue and its thermal response," *Proc. SPIE* **3914**, 511–516 (2000).
54. Q. Ye, J. Wang, Z.-C. Deng, W.-Y. Zhou, C. P. Zhang, J.-G. Tian, "Measurement of the complex refractive index of tissue-mimicking phantoms and biotissue by extended differential total reflection method," *J. Biomed. Opt.* **16**(9), 097001 (2011).
55. S. Cheng, H. Y. Shen, G. Zhang, C. H. Huang, X. J. Huang, "Measurement of the refractive index of biotissue at four laser wavelengths," *Proc. SPIE*, **4916**, 172–176 (2002).
56. G. J. Tearney, M. E. Brezinski, J. F. Southern, B. E. Bouma, M. R. Hee, J. G. Fujimoto, "Determination of the refractive index of highly scattering human tissue by optical coherence tomography," *Opt. Lett.* **20**(21), 2258–2260 (1995).
57. R. C. Haskell, F. D. Carlson, P. S. Blank, "Form birefringence of muscle," *Biophys. J.* **56**(2), 401–413 (1989).
58. A. N. Bashkatov, E. A. Genina, V. V. Tuchin, "Measurement of glucose diffusion coefficients in

human tissues," *Handbook of Optical Sensing of Glucose in Biological Fluids and Tissues*, Chapter 19, V. V. Tuchin (Ed.), pp. 587–621, Taylor & Francis Group LLC, CRC Press (2009).
59. W. Heller, Remarks on refractive index mixture rules, *J. Phys. Chem.* **69**(4), 1123–1129 (1965).
60. W. H. Press, S. A. Tuekolsky, W. T. Vettering, B. P. Flannery, *Numerical Recipes in C: The Art of Scientific Computing*, Cambridge University Press, Cambridge, New York (1992).
61. A. Kotyk, K. Janacek, *Membrane Transport: An Interdisciplinary Approach*, Plenum Press, New York (1977).
62. L. A. Alves, J. B. A. Silva, M. Giulietti, "Solubility of D-glucose in water and ethanol/water mixtures," *J. Chem. Eng. Data* **52**(6), 2166–2170 (2007).
63. R. C. Rowe, P. J. Sheskey, M. E. Quinn (Eds.), *Handbook of Pharmaceutical Excipients*, Pharmaceutical Press and American Pharmacists Association (2009).
64. Z. Zhu, G. Wu, H. Wei, H. Yang, Y. He, S. Xie, Q. Zhao, X. Guo, "Investigation of the permeability and optical clearing ability of different analytes in human normal and cancerous breast tissues by spectral domain OCT," *J. Biophotonics* **5**(7), 536–543 (2012).
65. Q. L. Zhao, J. L. Si, Z. Y. Guo, H. J. Wei, H. Q. Yang, G. Y. Wu, S. S. Xie, X. Y. Li, X. Guo, H. Q. Zhong, L. Q. Li, "Quantifying glucose permeability and enhanced light penetration in *ex vivo* human normal and cancerous esophagus tissues with optical coherence tomography," *Laser Phys. Lett.* **8**(1), 71–77 (2011).
66. K. Kretsos, M. A. Miller, G. Zamora-Estrada, G. B. Kasting, "Partitioning, diffusivity and clearance of skin permeants in mammalian dermis," *Int. J. Pharm.* **346**, 64–79 (2008).
67. H. Q. Zhong, Z. Y. Guo, H. J. Wei, C. C. Zeng, H. L. Xiong, Y. H. He, S. H. Liu, "Quantification of glycerol diffusion in human normal and cancer breast tissues *in vitro* with optical coherence tomography," *Laser Phys. Lett.* **7**(4), 315–320 (2010).
68. C. J. Goergen, H. Radhakrishnan, S. Sakadzic, E. T. Mandeville, E. H. Lo, D. E. Sosnovik, V. J. Srinivasan, "Optical coherence tractography using intrinsic contrast," *Opt. Lett.* **37**(18), 3882–3884 (2012).
69. J. L. Dashnau, N. V. Nucci, K. A. Sharp, J. M. Vanderkooi, "Hydrogen bonding and the cryoprotective properties of glycerol/water mixtures," *J. Phys. Chem.* **110**(27), 13670–13677 (2006).